Physica Scripta

PAPER

Annealing effect on cds nanowalls grown by chemical bath deposition on glass substrate

E Yildirim[1], S Ildan Ozmen[2], Ali Kemal Havare[3,4,*] and H Metin Gubur[1]

[1] Department of Physics, Mersin University, Mersin, Turkey
[2] Advanced Technology Education Research and Application Center, Mersin University, Mersin, Turkey
[3] Electric and Electronics Engineering, Photoelectronics Lab (PEL), Toros University, Mersin, Turkey
[4] Renewable Energy Technologies, Education, Research and Application Center (YETAM), Toros University, Mersin, Turkey
[*] Author to whom any correspondence should be addressed.

E-mail: alikemal.havare@gmail.com

RECEIVED
24 March 2023

REVISED
6 June 2023

ACCEPTED FOR PUBLICATION
12 June 2023

PUBLISHED
21 June 2023

Keywords: chemical bath deposition, SEM CdS films, annealing effect, conductivity, hall effect

Abstract

This paper focuses on the structural, morphological, and optical properties of the CdS thin films on the glass substrate with the effect of annealing. Chemical bath deposition (CBD) is a basic technique that is used in this work to form CdS thin films. The films′ (d) thickness is calculated to be 400 nm. According to the XRD results, the particle sizes for the as-deposited and the annealed CdS film are 15.15 nm and 16.56 nm, respectively. The SEM images of formed nanowalls in the films were compared for both the as-deposited and the annealed CdS structure. It was attained with the Raman spectroscopy analysis that as-deposited and annealed films include the LO phonon modes of the CdS. Moreover, FT-IR analysis was performed to determine the hydroxide ion (OH^-) behavior depending on the annealing effect. The optical band gap energy of the annealed CdS nanowalls reduced from 2.31 eV to 2.19 eV, according to the UV measurements. Additionally, the Hall Effect is used to assess the conductivity and resistivity of as-deposited and annealed films. This work demonstrated that CdS films readily form nanowalls at 85 °C.

1. Introduction

The semiconductor materials are used in many fields such as solar cell [1, 2], transistor [3], light emitting diode [4], lasers [5], photocatalyst [6], biosensor [7], biolabel [8]. In recent years, one of the prominent applications among the many application areas of these useful materials is solar cell applications. Considering the technological development of solar cells recently, the first generation is crystalline silicon, gallium arsenic solar cells and the second generation is thin films: CuInSe, CdTe, a-Si solar cells and finally third generation is dye sensitive solar cells, organic solar cells [9]. Cd based thin films have lately attracted great interest from the research community, with solar cells and other optoelectronic applications, and are used in the manufacture of solar cells due to the low band gap. CdS semiconductor thin films are obtained by various methods such as chemical deposition [10–15], electrodeposition [16], thermal evaporation [17], RF Magnetron sputtering [18], chemical spray pyrolysis [19]. Different CdS semiconductor morphologies have been prepared using various methods, including nanorods [20], flower-like nanorings [21], conifer-like [22], cauliflower-like microspheres [23], nanowires [24], flakes [25], and flowers [26]. Chemical vapor deposition, plasma assisted approach, microwave-based method, solution growth method and hydrothermal pathway methods come to the fore when focusing primarily on which techniques are used in the literature to create nanowalls. In particular, nanowall CdS structures could be fabricated by another methods that is microwave assisted chemical bath deposition [27] and sputter deposition technique [28]. However, among all these techniques, chemical bath deposition is a much simpler technique to obtain nanowalls. Research on nanowalls, from organic, inorganic materials to improve the stability and efficiency of surface reaction and is of interest today because of its simple method of synthesis, sometimes from a combination of both organic and inorganic materials. In general, nanowall

structures can have a unique shape, large surface area, and a two- or three-dimensional structure. These structures have both organic and inorganic chemical structures, including polymer nanowalls [29], graphene nanowalls [30], and carbon nanowalls [31–33] depending on the composition, the chemical structures of the nanowalls formations [34]. Inorganic nanowalls can be further divided into carbon-based and non-carbon-based nanomaterials. Graphene and carbon nanowalls structures are among the examples that can represent carbon-based nanowalls. Metal oxide and metal sulfide-based nanowalls make up the majority of non-carbon-based nanowalls. Direct-current plasma chemical vapor deposition is used to create carbon-based nanowalls on a silicon substrate [35]. The aforementioned approaches are well recognized as being extremely challenging procedures with intricate applications and precise control requirements. On the other hand, there are simple fundamental methods that are a sequential ionic layer adsorption and reaction-SILAR, and CBD. CBD technique is one of the easiest way is able to is applied to create non-carbon-based nanowalls [36]. In this study we prefer to perform the CBD method that has been carried out by many researchers to obtain CdS semiconductor thin film since it is straightforward and affordable to manage the growth rate, is homogeneous, and adheres to crystal structures. In accordance with the general reactions of the CBD method [37, 38], CdS semiconductor thin films can be deposited with different CBD method. Furthermore, the nanowall structures significantly enhance the surface area compared to the smooth thin films [27]. This can be advantageous in applications like solar cells and photodetectors, where interaction with light or other particles is key. The unique morphology of nanowall structures can enhance light absorption, making them excellent candidates for optoelectronic applications. Nanowall structures can potentially improve charge carrier transport due to their high-quality crystalline nature, which can help in reducing charge recombination and enhancing the efficiency of devices by efficient charge carrier transport in the device [39–41]. The dimensions of the nanowalls (like thickness, height, etc) can be tuned during the fabrication process, allowing control over their optical and electronic properties. CBD is a simple, inexpensive, and scalable technique, which can deposit thin films on large areas and different substrates. This makes the CdS nanowall structures a potentially viable choice for commercial applications.

We focused on CdS metal sulfide-based nanowalls in this paper. The effect of annealing on structural, optical, and electrical properties of the CdS nanowalls was studied. Using UV-Visible spectroscopy, the films' optical characteristics were obtained. The structural properties of CdS films were investigated using XRD, SEM, EDX, and FT-IR techniques. The CdS films, the crystal structure and crystal size by XRD, surface morphology and structure by SEM, chemical composition with EDS, and finally hydroxide ion (OH^-) behavior by FT-IR were determined. The Hall Effect method was used to measure the conductivity for the films and Raman spectroscopy analyzed the vibrational and structural characteristics of CdS films.

2. Preparation of CdS and measurements

Chemical bath deposition technique was used to obtain CdS thin films on glass surfaces at 85 °C. In the solution prepared to obtain the CdS semiconductor thin film by chemical bath deposition method, cadmium salts such as cadmium sulfate ($CdSO_4$), ammonia (NH_3), thiourea (SC (NH_2)$_2$) /hydrazine (N_2H_4) etc and ultrapure water. Hydrazine forms a complex with cadmium in the solution and the cadmium complex formed gives Cd^{2+} ion to the solution in a controlled manner. Ammonia is used to release S^{2-} ions from thiourea by forming OH^- ions in the aqueous medium. Thus, the ions released into the solution participate in the following reactions using the ion-ion mechanism to produce cadmium sulfide (CdS) on the substrate surface [1, 4, 5].

$$2NH_3 + 2H_2O \leftrightarrow 2NH_4^+ + 2OH^- \quad (1)$$

$$Cd(HN_3)_4^{2+} \leftrightarrow Cd^{2+} + 4NH_3 \quad (2)$$

$$SC(NH_2)_2 + 2OH^- \rightarrow S^{2-} + CN_2H_2 + 2H_2O \quad (3)$$

$$Cd^{2+} + S^{2-} \rightarrow CdS \quad (4)$$

A solution of 100 ml for the obtaining of CdS film of type n and nanowall structure; 0.2 M cadmium sulfate, 0.3 M thiourea, 1 M hydrazine, 25% ammonia, ultra-deionized water is composed of its components. Cadmium sulfate, thiourea, hydrazine, ammonia, and ultra-pure water; a clean beaker of 100 ml is constantly mixed with a clean glass bar and placed in order. This beaker was placed in a hot water bath inside the 500 ml beaker located on the heater. The two cleaned glass substrates were immersed into perpendicularly the solution with 9.4 pH when the temperature of the solution reaches 85 °C. The films are deposited on glass substrates for 35 min In order to measure the optical properties of the prepared CdS semiconductor thin films, the front part of the films formed on the two surfaces of the glass substrates was cleaned with 38% hydrofluoric acid (HF) of 0.5 M. The films were rinsed with deionized water and dried with cold air. Then it was rinsed with propanol and dried again. Thus, two nanowalls structured CdS semiconductor thin films were produced in a short time about 35 min at

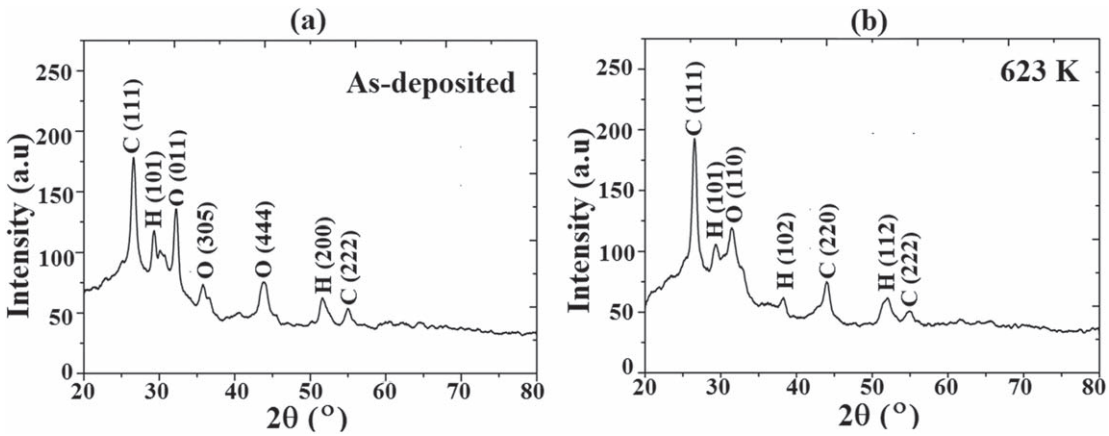

Figure 1. XRD pattern of the CdS nanowall films (a) as-deposited, and (b) annealed at 623 K in nitrogen atmosphere.

85 °C by CBD technique which is a straightforward and economical method. One of them was annealed in nitrogen atmosphere at 623 K for 1 h.

The structural analyses were performed utilizing the range of diffraction angles $20° \leqslant 2\theta \leqslant 80°$ in steps of 0.01° at 40 kV and 30 mA with $CuK_{\alpha 1}$ radiation ($\lambda = 1.5406$ Å) that available on a Rigaku Smart Lab x-ray diffractometer. A FEI-Quanta 650 Field Emission scanning electron microscope (SEM) that has an energy dispersive x-ray (EDX) spectrometer and a computer-controlled image analyzer was used to examine the surface morphology of the CdS nanowalls at different magnifications. Raman spectroscopy was conducted to understand the structural properties of CdS films, using a Renishaw inVia Qontor Raman microscope at 785 nm wavelength. The Fourier Transform-Infrared (FT-IR) spectra of the films were recorded by Jasco FT/IR-6700 in the wavelength range of 4000 to 500 cm^{-1}. Using the Shimadzu UV-1700, UV-visible spectrophotometer in the wavelength range of 300 to1100 nm at room temperature, the optical transmission spectra, and the thicknesses of the CdS nanowalls were calculated. The pH of the solution was measured with a Hanna Instruments HI 2211 pH/ORP Meter. The electrical properties of the films were measured by the Hall effect method which includes a Van der Pauw four-point probe configuration using gold contacts with a magnetic induction of 0.54 T at room temperature.

3. Results and discussion

3.1. Structural analysis

Assignments of cubic (C) (PDF Card No: 01-089-0440, 01-080-4441), hexagonal (H) (PDF Card No: 01-077-2306, 01-074-9664, 01-074-9665), orthorhombic (O) (PDF Card No: 01-082-4658, 00-047-1179) were created using standard JPDS (Joint Committee on Powder Diffraction Standards) cards. Plane indices were obtained by comparing the observed 'd' and '2-theta' values with the values on the cards. The as-deposited and annealed CdS nanowall films show mixed phases of hexagonal, orthorhombic, and cubic. According to the XRD graphs shown in figures 1(a) and (b), each peak value corresponding to 2-theta angles was compared, and it was found that the cubic and hexagonal structures were conserved in the C(111)-C(111), H(101)-H(101), and C(222)-C (222). The indices O(011)-O(110), O(305)-H(102), O(444)-C(220), and H(200)-H(112), however, all showed phase transitions.

By using the Debye–Scherrer formula $\left(D_{hkl} = \frac{K\lambda}{\beta \cos\theta}\right)$ to the full width at half maximum (FWHM) of the (111) peak for the cubic phase, the crystallite size of the CdS nanowalls was determined. Using the crystallite size found for CdS nanowalls, dislocation densities ($\delta = 1/D_{hkl}^2$), crystallite numbers per unit area ($N = d/D_{hkl}^3$) ($d = 400$ nm found in the 'Optical Properties' section), and strain values ($\varepsilon = \beta \cos\theta/4$) were determined and given in table 1 for the as-deposited and annealed CdS nanowall films. According to the data in the table calculated based on C(111) peak at $2\theta = 26.60°$, it was observed that the FWHM decreased, the particle size increased, the number of crystals per unit area, the dislocation density and the strain decreased with annealing [42]. The as-deposited CdS film's nanoparticle size is 15.15 nm, while the annealed films is 16.56 nm for C(111) according to the XRD data and these results are compatible with literature that the calculated crystallite size of CdS is found to be 20 nm for (111) plane [43]. High-temperature annealing is a technique commonly employed by researchers to eliminate the defects formed during thin-film deposition and improve crystal quality [8, 9]. Exposure to high temperatures during annealing removes the water molecules in the film (supported by FT-IR

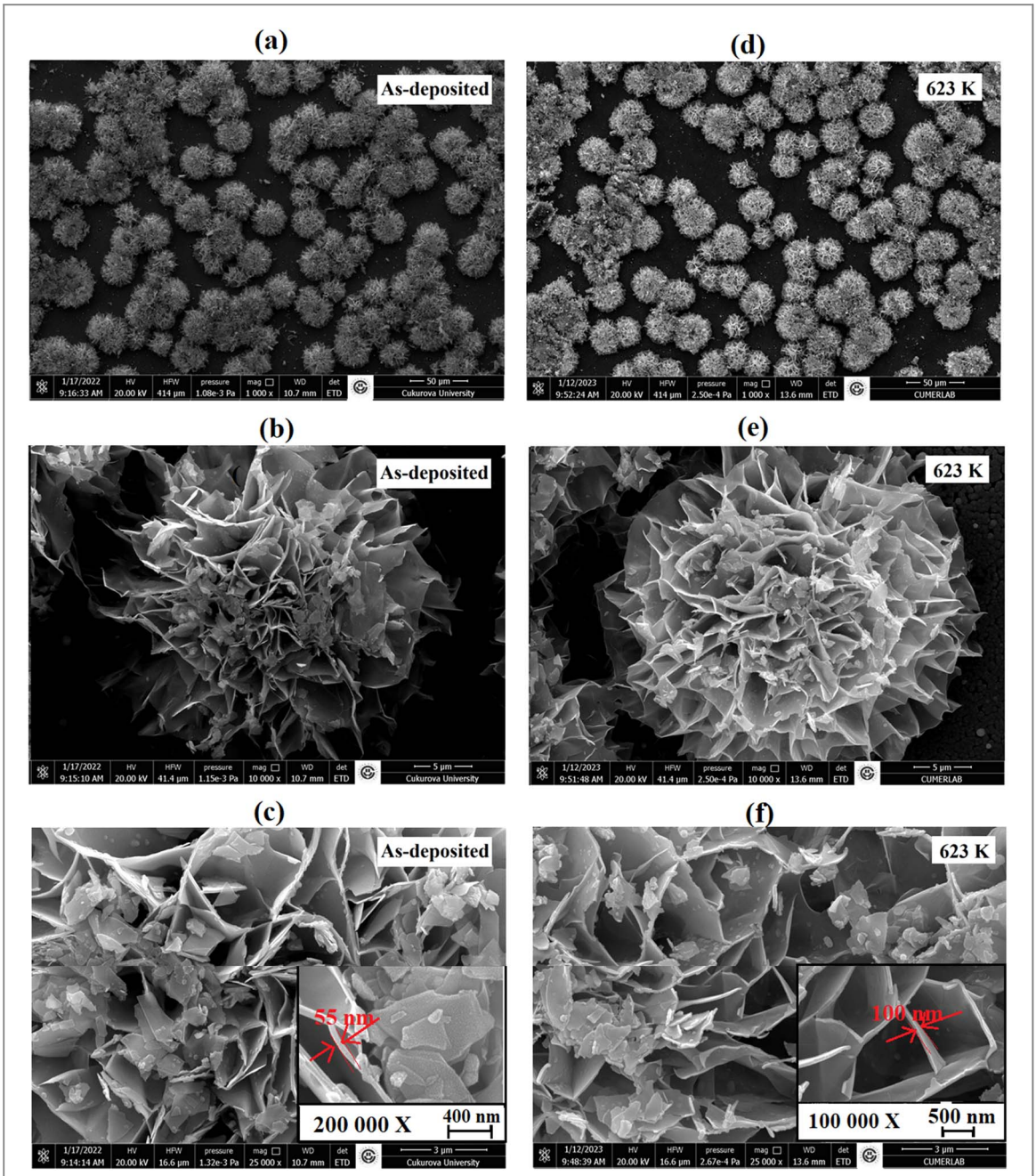

Figure 2. The SEM images of the as deposited and the annealed CdS nanowalls: (a) and (d) 1 000 X (b) and (e) 10 000 X and (c) and (f) 25 000 X magnification. The images at 200 000 X and 100 000 X magnifications are given respectively inset at (c) and (f).

Table 1. The FWHM, crystallite size, dislocation density, number of crystallites per unit area, and strain values for the as-deposited and annealed CdS films.

Nanowall glass/CdS	FWHM (rad)	D (nm)	δ (10^{15} lines/m^2)	N (10^{18} m^{-2})	ε (10^{-3})
As-deposited	0.0094	15.15	4.35	0.11	2.29
623 K	0.0086	16.56	3.65	0.088	2.09

analysis). In addition, the small crystals absorb heat and coalesce and recrystallize to form larger crystals. Therefore, the crystal size (D) increases as the FWHM decreases [9, 10].

Figures 2(a)–(f) shows the SEM images at different magnifications of the glass/CdS nanowalls that were as-deposited and annealed in a nitrogen atmosphere at 623 K. The low-dimensional image in figures 2(a) and (d) shows that the glass/CdS film surface is composed of porous nanowalls. Also, this film reveals nanowalls at magnifications of 10 000 X in figures 2(b) and (e), which resemble a particular variety of dahlia. Figure 2(c)

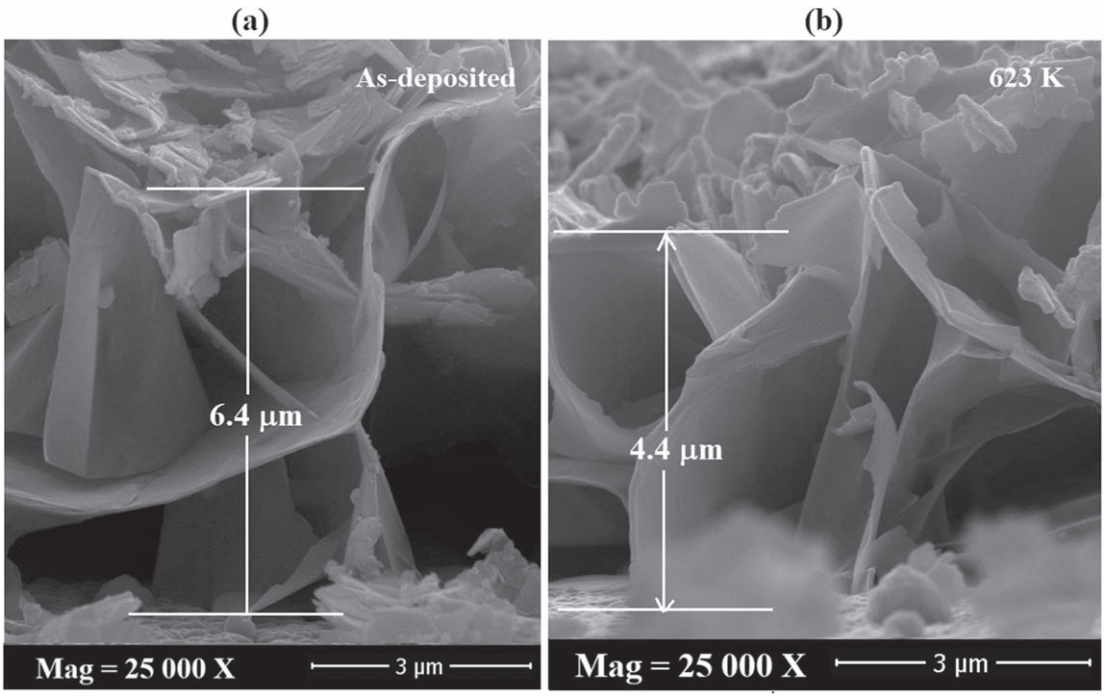

Figure 3. At 25 000 X magnification, SEM images of cross-sectional surfaces of the CdS nanowalls (a) as-deposited and (b) annealed.

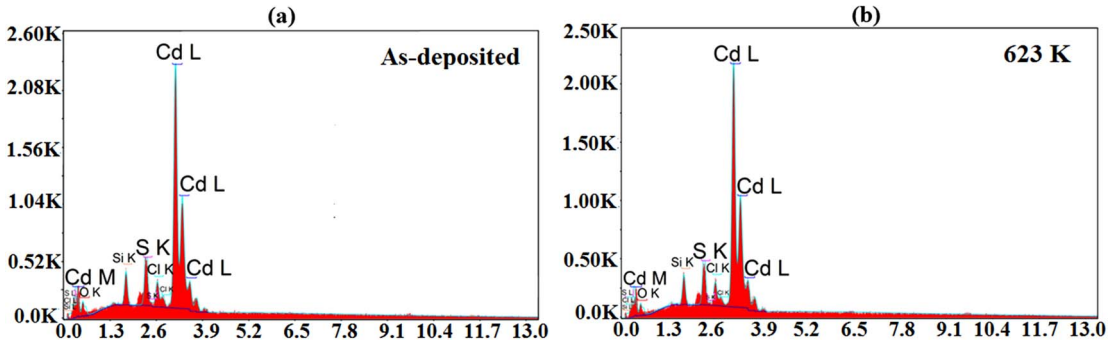

Figure 4. EDS analyzes of the as-deposited and the annealed CdS nanowalls.

appears to have particularly sharp-edged CdS nanowalls structures. Figures 2(c) and (f) at the 25 000 X magnifications exhibit CdS nanowalls forming nano channels that the nanowalls network is interconnected. As shown inset in figures 2(c)–(f) 200 000 X and 100 000 X magnification, the thickness of the as-deposited and annealed nanowalls was found to be ∼55 nm and ∼100, respectively. In the literature, the wall thickness is given as 70–100 nm. It is seen that our values are compatible with the literature [43] The surface of the nanowalls appears to be smooth.

Figure 3 shows SEM images of (a) as-deposited and (b) annealed cross-sectional surfaces of CdS nanowalls at 25 000 X magnification. The corresponding cross-sectional images show that the as-deposited and annealed nanowalls are well aligned with lengths of 6.4 μm and 4.4 μm respectively. Similar lengths have been reported in previous studies [44].

The ratio of element weights according to EDS analysis is shown in figure 4. As-deposited glass/CdS films have a Cd : S atomic ratio of 2.95 and annealed nanowalls glass/CdS films have a Cd : S atomic ratio of 3.44.

Raman spectroscopy is a powerful research technique used to analyze the vibrational and structural properties of materials. Raman spectroscopy was conducted to understand the structural properties of CdS films, using a Renishaw inVia Qontor Raman microscope at 785 nm wavelength. The Raman spectra of the as-deposited and annealed glass/CdS thin films are shown in figure 5 in the range of 250 cm^{-1} and 350 cm^{-1}. It was seen that peaks are broad in the spectrum. Broad peaks can be observed for amorphous or polycrystalline materials [44, 45] and we identified the films as polycrystalline by XRD analysis. The spectrum of as-deposited

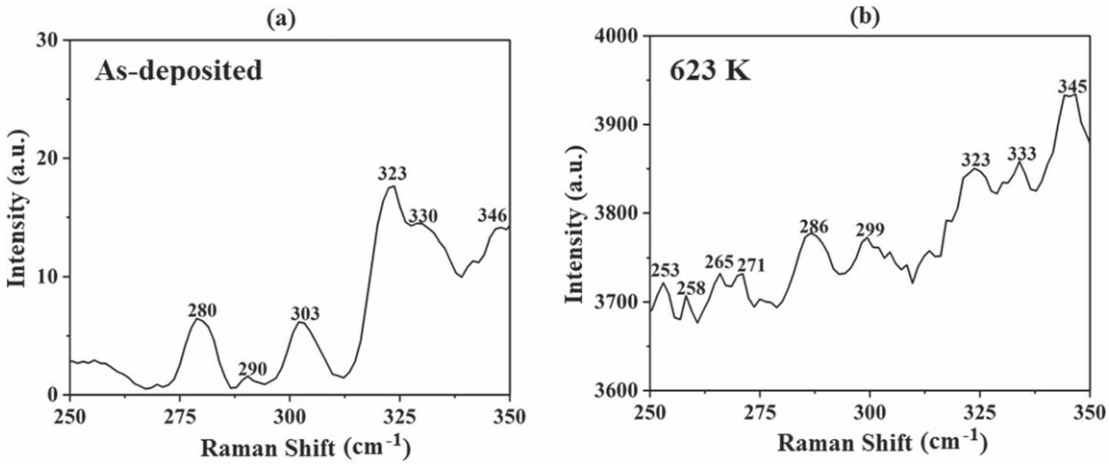

Figure 5. Raman spectra of (a) as-deposited and (b) annealed glass/CdS films.

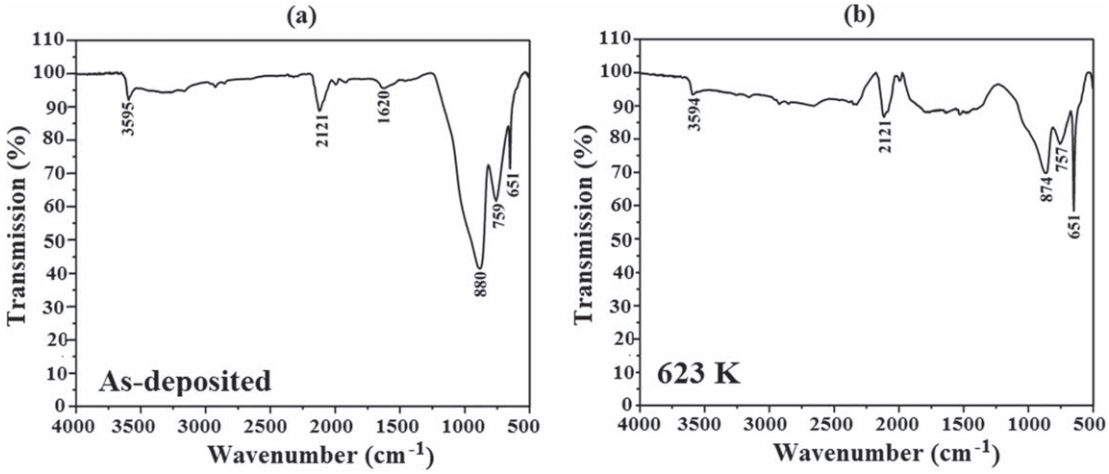

Figure 6. FT-IR spectra of CdS nanowalls (a) as-deposited and (b) annealed.

CdS thin film exhibits peaks around 280, 303, 323, 330, and 346 cm^{-1}. The Raman peaks at 280 cm^{-1} [46, 47] and 303 cm^{-1} [48, 49] correspond to the A1 longitudinal optical phonon (LO) modes of CdS. The other peaks are multi phonon scattering modes of CdS [47, 50]. The spectrum of annealed CdS thin film exhibits vibrations around 253, 258, 265, 271, 286, 299, 323, 333, 345 cm^{-1}. The A1 longitudinal optical phonon (LO) phonon modes of CdS are seen at 286 cm^{-1} and 299 cm^{-1} in the annealed CdS film. The phonon modes seen in the as-deposited CdS thin film, shifted from 280 cm^{-1} to 286 cm^{-1}, and from 303 cm^{-1} to 299 cm^{-1} in the annealed CdS thin film. The shifts in the Raman spectrum are attributed to the size effect or the surface optical phonon (SOP) mode effect. Surface phonon modes are observed for particle sizes smaller than the wavelength of exciting laser light inside the particles [51–54].

Figure 6 displays the FT-IR spectra of as-deposited and annealed CdS films. It has been observed that six peaks in as-deposited CdS film spectrum and five peaks in annealed CdS film spectrum. The peak at 3595(4) cm^{-1} is associated with the OH^- band stretching vibrations due to the intramolecular hydrogen bonds [1]. The peak at 2121 cm^{-1} belongs to the isothiocyanate (-NCS) which formed due to the hydrolysis of thiourea during the synthesis [6]. The peak at 1620 cm^{-1} is seen in the as-deposited CdS film disappeared with annealing and the peak intensity at 880 cm^{-1} decreased with annealing (874 cm^{-1}). These peaks are associated with the bending vibrations of H_2O molecules that out of plane [6, 7]. Finally, the peaks at 759 (757) cm^{-1} and 651 cm^{-1} are ascribed to the Cd-S stretching vibrations [6, 7].

3.2. Optical properties

The optical band gap determines the energy range of photons that can be absorbed by the semiconductor material. For solar cells, it is essential to match the energy conversion with the band gap energy of the absorber

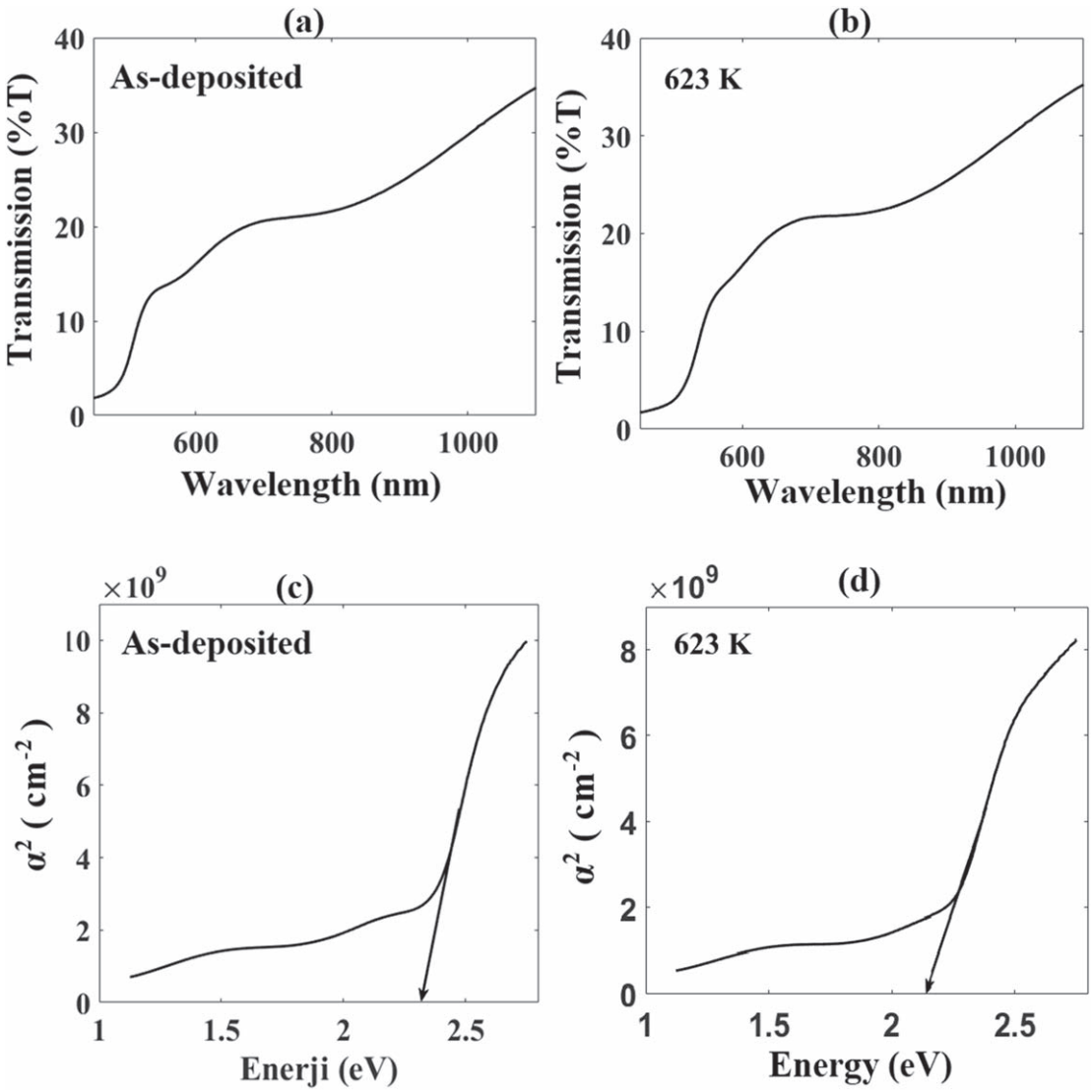

Figure 7. (a)–(b) Optical transmission spectrum and (c)–(d) α^2-$h\nu$ graph the CdS nanowalls of the as-deposited and annealed at 623 K.

material (CdS thin film). CdS has a relatively wide band gap in the range of 2.3 to 2.9 eV [45, 55, 56], which corresponds to the visible and near-ultraviolet region of the electromagnetic spectrum. This range allows efficient absorption, enhancing overall solar cell efficiency. The range of optical band gap values of CdS thin films is crucial for solar cell applications as it influences absorption, photovoltaic conversion efficiency, and effective device integration. Properly selecting the band gap within the suitable range enables CdS thin films to enhance solar cell performance and overall energy conversion efficiency. According to our results the transmission spectra of the 400–1100 nm wavelength range for the as-deposited and annealed CdS nanowalls are shown in figure 7. Because of the CdS's wide band gap, the CdS nanowalls absorbed light at a wavelength of roughly 500 nm. In our previous publications, we discussed the formulae used to calculate the thicknesses and absorption coefficients (α) of the films [14]. The thickness (d) of the film is calculated to be 400 nm. Figure 7 depicts these films' α^2 versus photon energy curves (c)–(d). The energy value for $\alpha^2 = 0$ is the optical band gap energy (Eg). The annealing caused the optical band gap energy of the CdS nanowalls to decrease from 2.31 to 2.19 eV in their as-deposited and annealed.

CdS films have been produced on different substrates by the CBD method based on temperature, pH and time control in literature [57]. According to these studies, polycrystalline n-type films with a forbidden energy gap of around 2.40 eV were obtained. In our study, similarly, nanowall-structured CdS semiconductor thin films were produced by CBD at 85 °C in a short time like 35 min One of the positive aspects of our study is that the cadmium molarity is quite low compared to the study of Vanalakar *et al* [43]. The pH of the solution is 9.4.

Table 2. Band gap (E_g), bulk concentration, mobility (μ), resistivity (ρ), conductivity (σ) and carrier type of the CdS nanowalls as-deposited and the annealed.

Annealing Temperature (K)	Bulk Concentration (cm^{-3})	Mobility (cm^2/Vs)	Resistivity (Ω-cm)	Conductivity $(\Omega\text{-cm})^{-1}$	Carrier Type
As-deposited	5.91×10^{10}	9.62×10^{3}	1.10×10^{4}	9.11×10^{-5}	n
623	5.60×10^{11}	51.67	2.15×10^{5}	4.63×10^{-6}	n

3.3. Electrical properties

The results of mobility and conductivity, which are two vital parameters for the electrical characterization of CdS thin films, have an impact on the performance of solar cells. By optimizing the mobility and conductivity of CdS thin films, solar cells can achieve improved power conversion efficiency, reliable operation, and enhanced overall performance. Based on this approach, the electrical characteristics of the CdS nanowall films are investigated at room temperature using a Hall Effect measuring set up with a Van der Pauw geometry. The following are the experimental procedures: Indium metal is soldered using the ohmic contacts attached to the four corners of the square-shaped CdS films. The magnetic field's magnitude and typical current carrying values were 0.54 Tesla and 1 mA, respectively. The Hall measurements of the CdS nanowall films in their as-deposited and annealed states are carried out repeatedly to ensure a certain reliability of the results. The results are shown in table 2. CdS nanowall films that have been as-deposited and annealed are n-type semiconductors. In CdS thin films, it was observed that the carrier density increased with annealing, leading to a decrease in mobility. However, the conductivity exhibited an inverse relationship with the carrier density, decreased as the carrier density increased. Comparing the conductivity of the annealed nanowalls film to the conductivity of the as-deposited nanowall film decreased from 9.11×10^{-5} $(\Omega\text{-cm})^{-1}$ to the 4.63×10^{-6} $(\Omega\text{-cm})^{-1}$. This may be because the concentration of the traps which result from nanowalls that appear by annealing and dominates trapped carrier becomes in critical level. Furthermore, the mobility of charge carriers in CdS thin films is influenced by temperature through various scattering mechanisms such as lattice scattering. As the temperature increases, these scattering mechanisms become more pronounced, resulting in decreased mobility. The conductivity of the CdS thin film aids in effectively separating the produced charge carriers during photovoltaic energy conversion, which enhances the efficiency of the solar cell when CdS thin film is utilized as a buffer layer in thin film solar cells.

4. Conclusion

In this paper the CdS nanowall thin films were produced on glass substrates with Cd^{2+} and S^2 ion sources included thiourea and cadmium sulfate by chemical bath deposition at 85 °C., Hydrazine and ammonia were used as agents. The glass/CdS film was annealed in nitrogen atmosphere at 623 K for a 1 h. The annealed CdS film has a particle size of 16.56 nm, whereas the as-deposited CdS film has a particle size of 15.15 nm, according to the X - ray diffraction patterns. The structures of both films are polycrystalline and consist of orthorhombic, hexagonal, and cubic phases. As a result, the strain, the number of crystallites/unit area, and the dislocation densities caused by crystal defects all reduced with annealing. The Cd-S stretching vibrations have been identified by FT-IR analysis and also it was seen that H_2O vibrations disappeared or decreased with annealing. We discovered that the semiconductor CdS thin films showed the nanowall structures through the SEM pictures. The optical band gap energy of the CdS nanowalls decreased from 2.31 to 2.19 eV with annealing according to UV measurements. Additionally, both resistivity and conductivity measurements were done utilizing the Hall effect approach. As a result, CdS nanowall thin films have strong electrical conductivity in addition to good optical and crystal quality, making them suitable for many applications such as solar cell applications.

Acknowledgments

This work was supported by grants of the Research Fund of Mersin University in Turkey with Project Number 2020-1-TP3-4032 BAP

Data availability statement

All data that support the findings of this study are included within the article (and any supplementary files).

Conflicts of interest

The authors declare no competing interests.

ORCID iDs

E Yildirim https://orcid.org/0000-0002-1540-9664
S Ildan Ozmen https://orcid.org/0000-0002-4222-0330
Ali Kemal Havare https://orcid.org/0000-0002-9272-9223
H Metin Gubur https://orcid.org/0000-0002-5796-5028

References

[1] Dolai S, Dey R, Hussain S, Bhar R and Pal A K 2019 Photovoltaic properties of F: SnO2/CdS/CuO/Ag heterojunction solar cell *Mater. Res. Bull.* **109** 1–9
[2] Majumder S, Mendhe A C and Sankapal B R 2019 Nanoheterojunction through PbS nanoparticles anchored CdS nanowires towards solar cell application *Int. J. Hydrogen Energy* **44** 7095–107
[3] Saha U and Alam M K 2019 A heterojunction bipolar transistor architecture-based solar cell using CBTSSe/CdS/ACZTSe materials *Sol. Energy* **184** 664–71
[4] Zhang Y, Zhang F, Wang H, Wang L, Wang F, Lin Q, Shen H and Li L S 2019 High-efficiency CdSe/CdS nanorod–based red light–emitting diodes *Opt. Express* **27** 7935–44
[5] Zhuang X, Ouyang Y, Wang X and Pan A 2019 Multicolor semiconductor lasers *Advanced Optical Materials* **7** 1900071
[6] Kavil J, Alshahrie A and Periyat P 2018 CdS sensitized TiO2 nano heterostructures as Sunlight driven photocatalyst *Nano-Structures & Nano-Objects* **16** 24–30
[7] Rathinamala I, Jeyakumaran N and Prithivikumaran N 2019 Sol-gel assisted spin coated CdS/PS electrode based glucose biosensor *Vacuum* **161** 291–6
[8] Tabrizi M A, Ferré-Borrull J, Kapruwan P and Marsal L F 2019 A photoelectrochemical sandwich immunoassay for protein S100β, a biomarker for Alzheimer's disease, using an ITO electrode modified with a reduced graphene oxide-gold conjugate and CdS-labeled secondary antibody *Microchim. Acta* **186** 1–9
[9] Can M, Havare A and Akan E 2021 Dye-sensitized solar cell (DSSC) applications based on cyano functional small molecules dyes *Int. J. Opt. Photonic Eng.* **6** 6
[10] Metin H, Erat S, Emen F, Kafadar V, Yazici A, Ari M and Kulcu N 2010 The thermoluminescence properties of CdS films under nitrogen atmosphere *J. Lumin.* **130** 1531–8
[11] Metin H, Ari M, Erat S, Durmuş S, Bozoklu M and Braun A 2010 The effect of annealing temperature on the structural, optical, and electrical properties of CdS films *J. Mater. Res.* **25** 189–96
[12] Metin H, Sat F, Erat S and Ari M 2008 Cadmium sulphide thin films grown by CBD: the effect of thermal annealing on the structural, electrical and optical properties *J. Optoelectron. Adv. Mater.* **10** 2622–30
[13] Metin H and Esen R 2003 Annealing studies on CBD grown CdS thin films *J. Cryst. Growth* **258** 141–8
[14] Metin H, Erat S, Durmuş S and Ari M 2010 Annealing effect on CdS/SnO2 films grown by chemical bath deposition *Appl. Surf. Sci.* **256** 5076–81
[15] Metin H and Esen R 2003 Annealing effects on optical and crystallographic properties of CBD grown CdS films *Semicond. Sci. Technol.* **18** 647
[16] Shen S, Zhang X, Mubeen S, Soriaga M P and Stickney J L 2019 Optimization of the nucleation-site density for the electrodeposition of cadmium sulfide on indium-tin-oxide *Electrochim. Acta* **316** 105–12
[17] Dey M, Das N, Gupta A S, Dey M, Hossain M, Matin M and Amin N 2019 Deposition of CdS thin film by thermal evaporation. *Int. Conf. on Electrical, Computer and Communication Engineering (ECCE). 2019. IEEE*
[18] Akcay N, Zaretskaya E and Ozcelik S 2019 Development of a CZTS solar cell with CdS buffer layer deposited by RF magnetron sputtering *J. Alloys Compd.* **772** 782–92
[19] Saleh K M 2019 Study influence of substrate temperature on optical properties of CdS thin films prepared by chemical spray pyrolysis *Ibn AL-Haitham Journal For Pure and Applied Sciences* **32** 7–16
[20] Qingqing W, Gaoling Z and Gaorong H 2005 Synthesis of single crystalline CdS nanorods by a PVP-assisted solvothermal method *Mater. Lett.* **59** 2625–9
[21] Song G, Zhang H, Li J, Peng Z, Xand L and Chen L 2012 Poly (vinyl-pyrrolidone) assisted hydrothermal synthesis of flower-like CdS nanorings *Polym. Bull.* **68** 2061–9
[22] Nan Y-X, Chen F, Yang L-G and Chen H-Z 2010 Electrochemical synthesis and charge transport properties of CdS nanocrystalline thin films with a conifer-like structure *J. Phys. Chem.* C **114** 11911–7
[23] Zhu Z, Wu Y, Liu H, Chen G and Zhu C 2013 Synthesis of CdS cauliflower-like microspheres via a template-free hydrothermal method *Mater. Lett.* **107** 90–2
[24] Kazeminezhad I, Hekmat N and Kiasat A 2014 Effect of growth parameters on structural and optical properties of CdS nanowires prepared by polymer controlled solvothermal route *Fibers Polym.* **15** 672–9
[25] Gao N and Guo F 2006 A hydrothermal approach to flake-shaped CdS single crystals *Mater. Lett.* **60** 3697–700
[26] Zhang H, Yang D and Ma X 2007 Synthesis of flower-like CdS nanostructures by organic-free hydrothermal process and their optical properties *Mater. Lett.* **61** 3507–10
[27] Abdulelah H, Ali B, Mahdi M, Hassan J, Al-Taay H and Jennings P 2017 Fabrication and characterization of nanowalls CdS/dye sensitized solar cells *Physica E* **90** 104–8
[28] Ilango M S and Ramasesha S K 2018 Novel patterning of CdS/CdTe thin film with back contacts for photovoltaic application *Pramana* **90** 1–8
[29] Gong J, Zhang W, Liu T and Zhang L 2011 Facile fabrication of chitosan–calcium carbonate nanowall arrays and their use as a sensitive non-enzymatic organophosphate pesticide sensor *Nanoscale* **3** 3123–31

[30] Zhang N, Li J, Liu Z, Yang S, Xu A, Chen D, Guo Q and Wang G 2018 Direct synthesis of vertical graphene nanowalls on glass substrate for thermal management *Mater. Res. Express* **5** 065606
[31] Ng H T, Li J, Smith M K, Nguyen P, Cassell A, Han J and Meyyappan M 2003 Growth of epitaxial nanowires at the junctions of nanowalls *Science* **300** 1249–1249
[32] Park W I, Lee C-H, Lee J M, Kim N-J and Yi G-C 2011 Inorganic nanostructures grown on graphene layers *Nanoscale* **3** 3522–33
[33] Hiramatsu M and Hori M 2010 Using carbon nanowalls as templates *Carbon Nanowalls* (Berlin: Springer) pp 131–57
[34] Kausar A 2022 State-of-the-art of polymer/nanowall nanocomposite: fundamental—to—leading-edge application *Polymer-Plastics Technology and Materials* **61** 665–81
[35] Tzeng Y, Chen W L, Wu C, Lo J-Y and Li C-Y 2013 The synthesis of graphene nanowalls on a diamond film on a silicon substrate by direct-current plasma chemical vapor deposition *Carbon* **53** 120–9
[36] Sankapal B, Mane R and Lokhande C 2000 Successive ionic layer adsorption and reaction (SILAR) method for the deposition of large area (∼ 10 cm2) tin disulfide (SnS2) thin films *Mater. Res. Bull.* **35** 2027–35
[37] Zhang S, Feng L, Li P, Zhang L, Chen X, Chu S, Gao Y, Xie S, Jiang J and Wang H 2021 *In situ* creation of ZnO@ CdS nanoflowers on ITO electrodes for sensitive photoelectrochemical detection of copper ions in blood *J. Mater. Chem.* B **9** 5869–76
[38] Mohamed H S, Rabia M, Shaban M and Taha S 2020 Controlled synthesis of CdS nanoflowers thin films for H2 electro-generation *Mater. Sci. Semicond. Process.* **120** 105307
[39] Yuan K, Chen L, Li F and Chen Y 2014 Nanostructured hybrid ZnO@ CdS nanowalls grown *in situ* for inverted polymer solar cells *J. Mate. Chem.* C **2** 1018–27
[40] Zhang W, Yang H, Li L, Lin S, Ji P, Hu C, Zhang D and Xi Y 2020 Flexible piezoelectric nanogenerators based on a CdS nanowall for self-powered sensors *Nanotechnology* **31** 385401
[41] Kumar D, Krishnan N S and Ramasesha S K 2022 Device simulation of nanopillar-based n-CdS/p-CdTe Solar Cell with enhanced and efficient carrier collection *Silicon* **15** 2037–43
[42] Khallaf H, Oladeji I O, Chai G and Chow L 2008 Characterization of CdS thin films grown by chemical bath deposition using four different cadmium sources *Thin Solid Films* **516** 7306–12
[43] Vanalakar S, Mali S, Jo E, Kim J, Kim J and Patil P 2014 Triton-X mediated interconnected nanowalls network of cadmium sulfide thin films via chemical bath deposition and their photoelectrochemical performance *Solid State Sci.* **36** 41–6
[44] Dhawale D, Dubal D, Deokate R, Gujar T, Sun Y and Lokhande C 2010 PVA assisted growth of hydrophobic honeycomb network of CdS thin films *J. Alloys Compd.* **503** 422–5
[45] Azmi N, Chelvanathan P, Yusoff Y, Shahahmadi S, Tiong S, Sopian K and Amin N 2020 A comprehensive study on the effects of alternative sulphur precursor on the material properties of chemical bath deposited CdS thin films *Ceram. Int.* **46** 18716–24
[46] Ballipinar F and Rastogi A 2017 High transmittance cadmium oxysulfide Cd (S, O) buffer layer grown by triton X-100 mediated chemical bath deposition for thin-film heterojunction solar cells *J. Appl. Phys.* **121** 035302
[47] Ahmed B, Kumar S, Kumar S and Ojha A K 2016 Shape induced (spherical, sheets and rods) optical and magnetic properties of CdS nanostructures with enhanced photocatalytic activity for photodegradation of methylene blue dye under ultra-violet irradiation *J. Alloys Compd.* **679** 324–34
[48] Isik M, Gullu H, Delice S, Parlak M and Gasanly N M 2019 Structural and temperature-dependent optical properties of thermally evaporated CdS thin films *Mater. Sci. Semicond. Process.* **93** 148–52
[49] Chun S, Jung Y, Kim J and Kim D 2011 The analysis of CdS thin film at the processes of manufacturing CdS/CdTe solar cells *J. Cryst. Growth* **326** 152–6
[50] Saleem M F, Zhang H, Deng Y and Wang D 2017 Resonant raman scattering in nanocrystalline thin CdS film *J. Raman Spectrosc.* **48** 224–9
[51] Trajić J, Gilić M, Romčević N, Romčević M, Stanišić G, Hadžić B, Petrović M and Yahia Y 2015 Raman spectroscopy of optical properties in CdS thin films *Sci. Sinter.* **47** 145–52
[52] Gilic M, Trajic J, Romcevic N, Romcevic M, Timotijevic D, Stanisic G and Yahia I 2013 Optical properties of CdS thin films *Opt. Mater.* **35** 1112–7
[53] Saxena N, Kalsi T, Uttam P and Kumar P 2018 Morphological evolution in nanocrystalline CdS thin films from flowers to salt rock like structures *Opt. Mater.* **84** 625–30
[54] Ren T, Lei Z, Luan G, Jia G, Zhang J, Yu R and Li C 2006 Fabrication of CdS–ZnS layered thin films by hydrothermal seeded growth method *Thin Solid Films* **513** 99–102
[55] Herrera-Molina D, Diosa J, Fernández-Pérez A and Mosquera-Vargas E 2021 Influence of aluminum doping on structural, morphological, vibrational, and optical properties of CdS thin films obtained by chemical bath deposition *Materials Science and Engineering:* B **273** 115451
[56] Chandekar K V, Shkir M, Khan A and AlFaify S 2020 An in-depth study on physical properties of facilely synthesized Dy@ CdS NPs through microwave route for optoelectronic technology *Mater. Sci. Semicond. Process.* **118** 105184
[57] Kaur I, Pandya D and Chopra K 1980 Growth kinetics and polymorphism of chemically deposited CdS films *J. Electrochem. Soc.* **127** 943